


# Shortening of time-to-peak left ventricular pressure rise (Td) in cardiac resynchronization therapy

Hans Henrik Odland<sup>1,2\*</sup> , Manuel Villegas-Martinez<sup>3</sup>, Stian Ross<sup>1</sup>, Torbjørn Holm<sup>1</sup>, Richard Cornelussen<sup>4</sup>, Espen W. Remme<sup>3,5</sup> and Erik Kongsgard<sup>1</sup>

<sup>1</sup>Department of Cardiology, Oslo University Hospital, Rikshospitalet, Oslo, 0027, Norway; <sup>2</sup>Department of Pediatric Cardiology, Oslo University Hospital, Oslo, 0027, Norway; <sup>3</sup>Intervention Center, Oslo University Hospital, Rikshospitalet, Oslo, 0027, Norway; <sup>4</sup>Bakken Research Centre, Medtronic Plc, Maastricht, The Netherlands; <sup>5</sup>Institute for Surgical Research, Oslo University Hospital, Rikshospitalet, Oslo, 0027, Norway

## Abstract

**Aims** We tested the hypothesis that shortening of time-to-peak left ventricular pressure rise (Td) reflect resynchronization in an animal model and that Td measured in patients will be helpful to identify long-term volumetric responders [end-systolic volume (ESV) decrease >15%] in cardiac resynchronization therapy (CRT).

**Methods** Td was analysed in an animal study ( $n = 12$ ) of left bundle-branch block (LBBB) with extensive instrumentation to detect left ventricular myocardial deformation, electrical activation, and pressures during pacing. The sum of electrical delays from the onset of pacing to four intracardiac electrodes formed a synchronicity index (SI). Pacing was performed at baseline, with LBBB, right and left ventricular pacing and finally with biventricular pacing (BIVP). We then studied Td at baseline and with BIVP in a clinical observational study in 45 patients during the implantation of CRT and followed up for up to 88 months.

**Results** We found a strong relationship between Td and SI in the animals ( $R = 0.84$ ,  $P < 0.01$ ). Td and SI increased from narrow QRS at baseline (Td =  $95 \pm 2$  ms, SI =  $141 \pm 8$  ms) to LBBB (Td =  $125 \pm 2$  ms, SI =  $247 \pm 9$  ms,  $P < 0.01$ ), and shortened with biventricular pacing (BIVP) (Td =  $113 \pm 2$  ms and SI =  $192 \pm 7$  ms,  $P < 0.01$ ). Prolongation of Td was associated with more wasted deformation during the preejection period ( $R = 0.77$ ,  $P < 0.01$ ). Six patients increased ESV by  $2.5 \pm 18\%$ , while 37 responders (85%) had a mean ESV decrease of  $40 \pm 15\%$  after more than 6 months of follow-up. Responders presented with a higher Td at baseline than non-responders ( $163 \pm 26$  ms vs.  $121 \pm 19$  ms,  $P < 0.01$ ). Td decreased to  $156 \pm 16$  ms ( $P = 0.02$ ) with CRT in responders, while in non-responders, Td increased to  $148 \pm 21$  ms ( $P < 0.01$ ). A decrease in Td with BIVP to values similar or below what was found at baseline accurately identified responders to therapy (AUC 0.98,  $P < 0.01$ ). Td at baseline and change in Td from baseline was linear related to the decrease in ESV at follow-up. All-cause mortality was high among six non-responders ( $n = 4$ ), while no patients died in the responder group during follow-up.

**Conclusions** Prolongation of Td is associated with cardiac dyssynchrony and more wasted deformation during the preejection period. Shortening of a prolonged Td with CRT in patients accurately identifies volumetric responders to CRT with incremental value on top of current guidelines and practices. Thus, Td carries the potential to become a biomarker to predict long-term volumetric response in CRT candidates.

**Keywords** Cardiac resynchronization therapy; Time-to-peak dP/dt; Reverse volumetric remodelling

Received: 22 April 2021; Revised: 29 July 2021; Accepted: 19 August 2021

\*Correspondence to: Hans Henrik Odland, Department of Pediatric Cardiology and Department of Cardiology, Oslo University Hospital, Rikshospitalet, 0027 Oslo, Norway.

Phone: +47 90509944. Email: hanshenrikodland@gmail.com

The work was performed at Oslo University Hospital, Department of Cardiology.

## Introduction

Cardiac resynchronization therapy (CRT) is beneficial to selected patients with a wide QRS complex and heart failure with improving survival rates, yet underutilized.<sup>1–3</sup> Left bundle branch block in non-ischaemic cardiomyopathy is typically

associated with better response, while unspecific conduction delay and ischaemic cardiomyopathy are associated with less beneficial effects,<sup>4</sup> and CRT may increase and decrease mortality in different subpopulations.<sup>5,6</sup> Only targeting subgroups with a higher likelihood of response may come at the cost of not treating patients with potential benefit, and targeting all

patients with widened QRS complex will likely burden patients with detrimental effects.<sup>7,8</sup> Therefore, it is of utmost importance to find selection criteria with incremental value beyond current guidelines to select suitable patients for CRT.<sup>9</sup> We aimed to analyse time-to-peak left ventricle (LV) dP/dt, and Td in animals and patients. We used the animal model to test how the left ventricle (LV) regional mechanical deformation and the LV electrical activation sequences affect Td. Td was then tested in an observational study in 45 patients to analyse the incremental value of Td on top of current selection criteria to detect patients with a beneficial response to CRT. With the data presented, we suggest that shortening of time-to-peak-LV dP/dt, Td, reflect disease modification in dyssynchronous heart failure (dysHF) and that Td has the potential to serve as a biomarker for the selection of patients amenable to CRT. One part presents animal data, and one part presents acute and long-term follow-up data on 45 patients with Td measurements before and after receiving a CRT device.

## Methods

### The experimental large animal study

#### *Animal preparation*

Twelve mongrel dogs of either sex were anaesthetized (single-dose methadone, 0.2 mg/kg; followed by propofol, 3 to 4 mg/kg, and a bolus of fentanyl, 2 to 3 mg/kg; thereafter, continuous infusion of propofol, 0.2 to 1 mg/kg/min, and fentanyl, 5 to 40 mg/kg/h). The animals were ventilated and surgically prepared with an open chest, as previously described.<sup>10</sup> We placed pacing electrodes in the right atrium and the endocardial RV septum/apex (RV<sub>apex</sub>). We placed LV pacing electrodes on the epicardial free wall in apical, anterior, and lateral areas. A cardiac pressure catheter and a catheter for radiofrequency ablation were introduced through peripheral vessel incisions. LV pressure was measured using a 5F micromanometer-tipped catheter (model MPC 500, Millar Instruments, Inc., Houston, Texas, USA). Radiofrequency ablation was performed with a standard ablation catheter (Celsius, Biosense Webster Inc., California, USA), targeting left bundle branch potentials to split the QRS complex and extend QRSd to above 100 ms.<sup>11</sup> LV dimensions and intramyocardial electrograms (EGM) were measured and collected using 2-mm sonomicrometric crystals. The crystals included electrodes (Sonometrics Corp., London, Ontario, Canada) and were implanted subendocardial in the equatorial plane in the interventricular septum, posterior, anterior, and lateral LV walls. Combined crystals with electrodes enabled the simultaneous evaluation of myocardial electrical and mechanical activation. We sampled data at 1 kHz and analysed recorded data in the LabChart Pro 8.0 software

(ADInstruments LTD, Oxford, UK). The Norwegian Food Safety Authority approved the study. The Center for Comparative Medicine (Oslo University Hospital, Rikshospitalet, Oslo, Norway) supplied the animals.

#### *Pacing interventions*

Atrial pacing (AP) was performed at a rate 10% above sinus rhythm at baseline with narrow QRS and after ablation with the induction of LBBB. Sequential biventricular pacing was then delivered with a paced AV-delay set between 30 and 60 ms to avoid fusion with intrinsic RV conduction. Pacing was performed from the right ventricle (RV), left ventricle (LV), and combined as biventricular (BiV) pacing in random order resulting in repeated measurements. Four measurements were excluded due to incomplete LBBB at baseline and LBBB-capture with RV septal pacing.

#### *Wasted deformation and synchronicity index*

Deformation was measured as the sum of *absolute* length changes in septal-lateral and anterior–posterior electrode pairs, both shortening and lengthening, from the onset of QRS complex or ventricular pacing until peak LV dP/dt (*Figure 1A and B*). We regarded deformations during this ideally iso (volu)metric period as wasted, representing dyssynergistic contractions.<sup>12</sup> We calculated the Synchronicity index (SI) as the sum of all intervals from pacing onset to local EGMs in the four equatorial electrodes (*Figure 1D*).

#### *Pacing stimulus to ventricular capture latency*

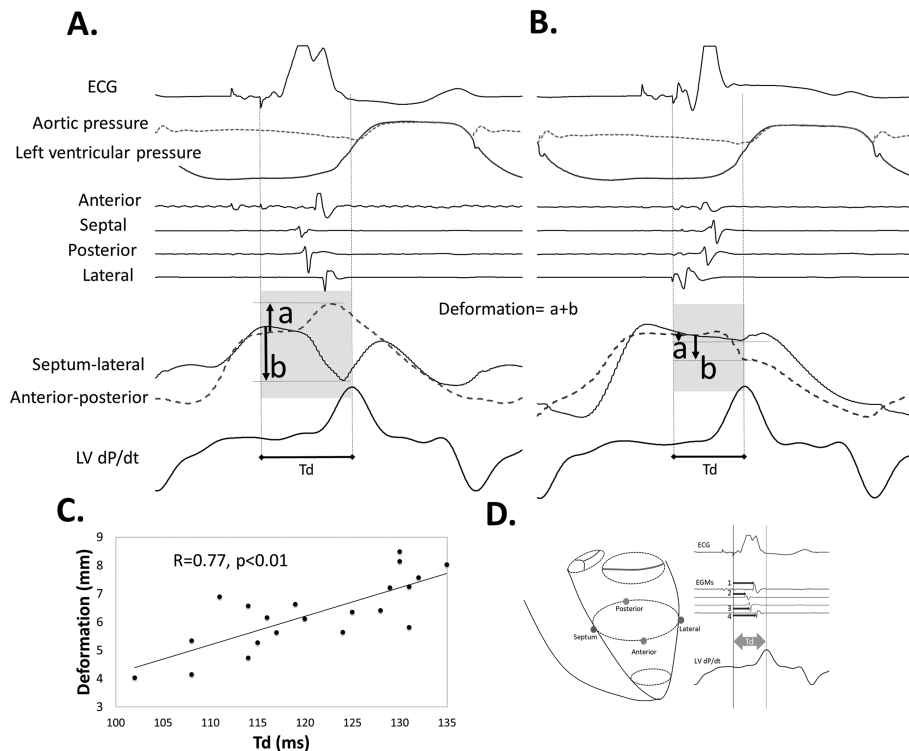
We aligned EGMs and QRS complexes from two representative beats, with similar QRS morphology and EGMs (intrinsic left bundle branch block (LBBB) and RV paced), in the animals to analyse the delay from ventricular pacing to ventricular capture (onset of QRS). We found a 15 ms delay from the beginning of the pacing spike to the start of QRS, consistent with the individual delays measured throughout the experiments. For comparison of activation timing between paced and native conduction, we added 15 ms to native conduction.

## Clinical observational study

#### *Study population*

Forty-five heart failure patients admitted for CRT implantation according to 2013 ESC guidelines were included in two different acute observational studies approved by the Regional Committees for Medical and Health Research Ethics in Norway and conducted following the principles of the Declaration of Helsinki. We obtained written, informed consent from all patients. Inclusion criteria were sinus rhythm, New York Heart Association functional class II and III heart failure on optimal medical therapy, left bundle branch block morphology,<sup>13</sup> QRS duration (QRSd) larger than 130 ms, and a left ventricular ejection fraction <35%. Exclusion criteria were age <18 years and above 80 years, ongoing atrial

**Figure 1** Regional myocardial deformation, relationship towards time-to-peak LV dP/dt, Td, and synchronicity index (SI). (A) Regional myocardial deformation with right ventricular (RV) free wall pacing. The electrical activation sequence is early in the septal electrode and last in the lateral. Lengthening occurs between anterior–posterior crystals and shortening between the septal and lateral crystals (septal beaking). This deformation represents a transfer of forces from one region to the other and indicates dyssynergy of contraction. Hence, more deformation equals more dyssynergy of contraction. Tension builds up with completion of electrical activation with rebound lengthening in the septal-lateral crystal pair before peak LV dP/dt and aortic valve opening. Total deformation is calculated as the sum of absolute maximum deformation values measured from the onset of pacing to peak LV dP/dt (A and B) and is limited to the isovolumetric period. (B) BIVP with RV apex and left ventricular (LV) lateral electrodes. The activation sequence is early lateral and late septal. Only minimal deformations occur (less dyssynergy) while tension increases towards the end of electrical activation up to peak LV dP/dt that occur early due to improved synergy from stimulation. (C) We found a linear relationship between Td and the total deformation, as measured between each pair of crystals (panel A and panel B), indicating that more deformation delays Td. (D) Synchronicity index (SI, ms) was constructed based on the sum of the four intervals 1–4 from the onset of pacing to the deflections in the respective equatorial EGMs (absolute dV/dt). BIVP, biventricular pacing; RV, right ventricle; dP/dt, left ventricular pressure derivative.



fibrillation and complete atrioventricular block. All patients had *de novo* implants. An echocardiogram was performed in all patients prior to implantation and after more than 6 months of follow up. Biplane Simpson auto EF (Echopac, GE Healthcare, Horten, Norway) was used for intracardiac systolic and diastolic volumes and EF.

#### Device implantation and intervention

Device implantation (CRT devices from Medtronic Inc. Fridley, Minnesota, USA) followed a standard left subclavian approach with a subcutaneous pocket. The RV lead was positioned in the apical endocardial portion of the right ventricle, while the LV lead (Attain Performa [4298, 4398, 4598], Medtronic Inc. Fridley, Minnesota, USA) was placed epicardial in a (postero-)lateral branch of the coronary vein in all patients. All positions were confirmed by biplane fluoroscopic imaging and later cross-registered on a fitted generic heart model. Bipolar pacing was performed in an

atrioventricular synchronized fashion with a fixed AV-delay for each patient to ensure proper biventricular stimulation. Confirmation of capture was carried out by visual inspection of the surface ECG. The heart rate was set at 10% above the intrinsic rate in sinus rhythm, and intrinsic AV-delay was measured. The paced AV-delay was set to <80% of the intrinsic AV-interval. Sequential biventricular pacing (BIVP) was performed with the EPS 320 cardiac stimulator (Micropace EP Inc., Santa Ana, CA, USA) connected to the implanted leads with alligator clips. A 3.5 Fr pressure sensor catheter (Micro-Cath™, Millar Instruments Inc., Houston, Texas, USA) was positioned through a 6 Fr delivery catheter from the right femoral artery to the left ventricular cavity. Heparin was given as a bolus of 100 IE/kg IV.

#### Data acquisition

Electrophysiology signals and ECGs were collected with the BARD Pro EP recording system and the Clearsign Amplifier

(Boston Scientific Inc., Marlborough, Massachusetts, USA). The left ventricle's pressure was measured with the Micro-cath pressure catheter and the PCU-2000 Pressure Control Unit (Millar Instruments Inc., Houston, Texas, USA). All signals were transferred in real-time from the recording system to a data acquisition unit (PowerLab, ADInstruments LTD, Oxford, UK), with each event logged for later analyses in the LabChart Pro 8.0 software (ADInstruments LTD, Oxford, UK). Pressures were then filtered with a low-pass filter of 15 Hz to remove noise. Time was given for the pressures to stabilize when pacing was performed before recording the data. QRS onset was marked as the first fluctuation above the isoelectric line, resulting in a complete QRS complex. Td was measured as the average of the time interval between QRS onset or pacing onset and peak of dP/dt on 6–8 subsequent beats after full capture of both atrium and ventricle. We used the leading edge of the first deflection of the stimulus artefact as a reference for pacing. The stimulus to capture latency creates a bias when comparing time from QRS onset and time from pacing spike to peak dP/dt. We corrected Td measured at baseline by adding the 15 ms delay seen from pacing stimulus to myocardial activation. We subsequently analysed latency from pacing to QRS onset in all patients and found a mean of  $14.0 \pm 2.1$  ms. A corrected change from baseline (Td) was then calculated as the difference between the measured value with BIVP and the corrected baseline value of Td. When not presented as corrected, Td is presented without correction. We measured beat to beat variation in Td with pacing in one patient and found a standard deviation from 18 beats within each pacing mode between 4 and 7 ms.

### Follow-up

Programming of the device, including selecting the LV pacing electrode, was carried out at the physicians' discretion. At a follow-up of more than 6 months, patients were classified as volumetric responders or volumetric non-responders with a cut-off at a 15% reduction in ESV.

### Statistical analysis

Linear mixed models (IBM SPSS 26.0, Armonk, New York) were used for the repeated measurements with compound symmetry as covariance type for both fixed and random effects, with each subject selected as random effects in both the animal and clinical studies.<sup>14</sup> We used the Hotelling Lawley Test and the GLIMMPSE sample size calculator (Glimmpse 3.0.0 (samplesizeshop.org)) to confirm power >80% for a Type I error of 5%. This statistical model takes individual differences into account for repeated measurements. The model with the lowest Akaike's information criteria was chosen when covariates were added to the models. The model output gives estimated marginal means for each fixed effect group when random effects and covariates are considered. A comparison was performed between

each group or combinations of them and a reference. Numbers from comparisons with mixed or general linear statistical models are estimated marginal mean  $\pm$  SEM, and those from descriptive statistics are mean  $\pm$  SD. A *P*-value of <0.05 was considered statistically significant. Receiver-operating characteristics curves were generated.

## Results

### Experimental study

QRSd, SI, and Td increased with AP-LBBB, RVP, and LVP compared with AP with normal conduction (Table 1). QRSd, SI and Td shortened with BIVP compared with AP-LBBB and RVP, and QRSd and Td shortened with BIVP compared with LVP (Table 1). We observed dyssynergistic deformations during the isovolumetric period as well as a delay in Td with RVP (Figure 1A). Resynchronization reduced dyssynergy and shortened Td (Figure 1B). Figure 1C shows the relationship between Td and the equatorial plane deformation with LBBB, RVP, and BIVP and confirmed the relationship between dyssynergy and Td. Figure 2 displays pressures, segment lengths, EGMs, and ECGs with intrinsic LBBB conduction and BIVP, as acquired in the experiments. It can be seen how EGMs become synchronous, deformation is reduced, and Td shortens with BIVP. Lastly, a strong, linear relationship was found both between QRSd and SI ( $\beta = 0.27$ ,  $R = 0.86$ ,  $P < 0.01$ ) and between Td and SI (Figure 3A), with good agreement between the two (Figure 3B), while there was a relatively weak relationship between LV dP/dt<sub>max</sub> and SI (Figure 3C). Td was associated with left ventricular electrical delay (Q-LV) to the lateral electrode (Q-LV lateral) when measured with narrow QRS, with LBBB and RV pace combined (Figure 3D).

**Table 1** Animal experiments (*n* = 12)

Mode of pacing	QRSd (ms)	SI (ms)	LV dP/dt <sub>max</sub> (mmHg/s)	Td (ms)
AAI (narrow QRS)	$70 \pm 2^{\dagger}$	$141 \pm 8^{\dagger}$	$1483 \pm 85^{\dagger}$	$95 \pm 2^{\dagger}$
AAI (LBBB)	$110 \pm 3$	$247 \pm 9^{\ddagger, \S}$	$1115 \pm 95$	$125 \pm 2$
DDD (RV)	$110 \pm 3$	$265 \pm 10^{\ddagger, \S}$	$1103 \pm 99$	$129 \pm 2^{\dagger}$
DDD (LV)	$103 \pm 2$	$214 \pm 6$	$1161 \pm 78$	$119 \pm 2$
DDD (BIV)	$87 \pm 2^{\dagger}$	$192 \pm 7$	$1232 \pm 84$	$113 \pm 2^{\dagger}$

AP, atrial pace; AP-LBBB, atrial pace with left bundle branch block; BIVP, biventricular pace; LVP, left ventricular pace; QRSd, QRS duration; RVP, right ventricular pace; SI, synchronicity Index; Td, time-to-peak LV dP/dt.

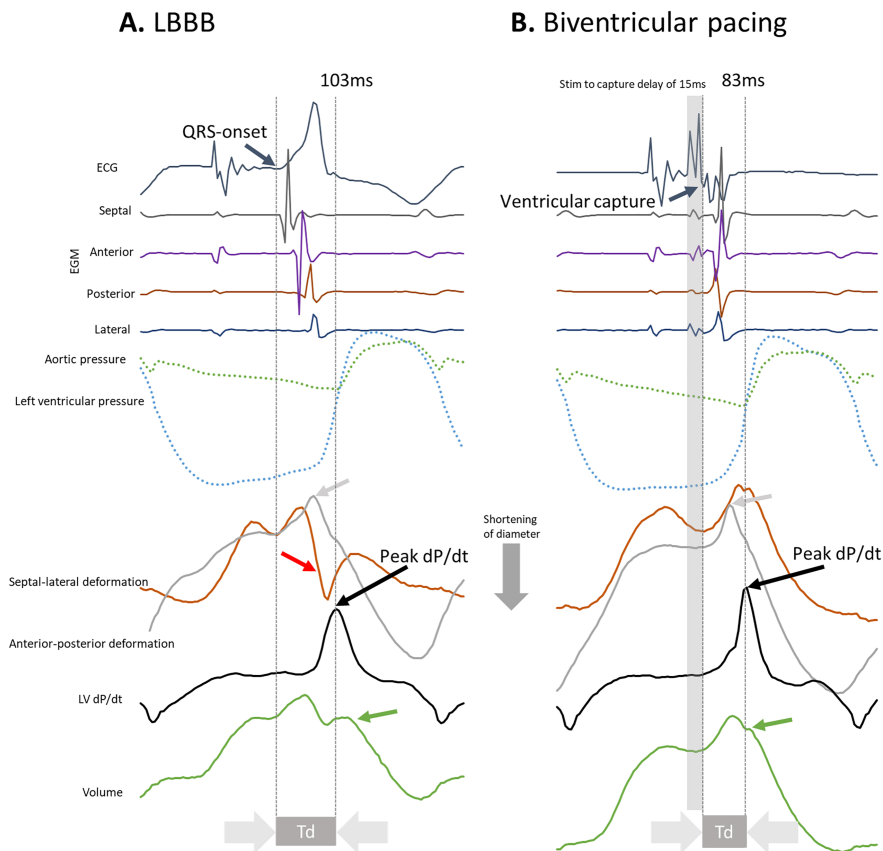
Electrophysiological and mechanical characteristics. The top five rows are compared (*n* = 12).

<sup>†</sup>*P* < 0.05 compared with all.

<sup>‡</sup>*P* < 0.05 compared with LVP.

<sup>§</sup>*P* < 0.05 compared with BIVP.

**Figure 2** Demonstration of shortening of time-to-peak dP/dt (Td) with biventricular pacing and myocardial synergy with simultaneous pacing of the RV and the LV (resynchronization). (A) Left bundle branch block (LBBB) with electrical activation patterns showing a sequence of septal-anterior-posterior-lateral activation with dyssynergistic septal and lateral wall contraction patterns with pressure rise reaching its peak just before aortic valve opening. Red arrow: Septal beaking. Grey arrow: shortening of the lateral segment. Green arrow: onset of ejection. (B) Biventricular pacing from an apical positioned left ventricular epicardial electrode demonstrates a simultaneous sequence of activation with synergistic septal and lateral wall contraction patterns and peak left ventricular pressure rise (that occur before aortic valve opening). Grey arrow: shortening of the lateral segment. Green arrow: onset of ejection. V1, ECG lead; RV, right ventricle; LV, left ventricle; LVP, left ventricular pressure; LV dP/dt, LV pressure derivative; Td, time-to-peak LV dP/dt.



## Clinical observational study

A lateral vein was targeted in all patients for LV stimulation (Supporting Information, *Figure S1A*), and anterolateral, lateral and posterolateral (mid and basal) segments were final LV lead positions Supporting Information, *Figure S1B*). All patients received maximal tolerated optimal medical therapy with either ACE inhibitor/ARB and/or beta-blocker with no significant differences between the groups (*Table 2*).

### Synergy from biventricular stimulation

*Figure 4* shows how Td prolongs with RV pace and shortens with LV pace compared with baseline AP; however, pacing from the RV and the LV combined shorten Td beyond what is seen with pacing from either of the electrodes (synergy from biventricular stimulation).

### Follow-up

During the study period with up to 88 months (range 16–88 months) follow-up, four patients (non-responders) died (one after heart transplant), and one patient (responder) with familial dilated cardiomyopathy underwent heart transplantation. The overall survival was estimated to  $81 \pm 3$  months with a significant difference in estimated survival between the non-responders at  $35 \pm 7$  months and responders  $86 \pm 1$  months ( $P < 0.01$ ) (Kaplan–Meier curve in Supporting Information, *Figure S1C*).

### Cardiac resynchronization therapy response

We found six non-responders with an ESV reduction  $<15\%$  at follow-up with a mean ESV increase of  $2.5 \pm 7\%$ . The remaining 37 responders had a mean ESV decrease of  $40 \pm 15\%$ . A comparison of volumes and ejection fraction between the groups is found in *Table 3*.



**Figure 3** Correlations between Td and synchronicity index (SI) with Bland–Altman plot and Td and LV dP/dt<sub>max</sub>. (A) A strong positive relationship was found between Td and SI in the animals with all pacing modes and intrinsic conduction with narrow QRS and LBBB pooled. (B) We divided SI by four since it is made up of four numbers to avoid a bias with higher numbers for the creation of the Bland–Altman plot against Td with limits of agreement. The plot indicates that the two methods reflect the same underlying pathology within limits of agreement with a bias of 64.45 ms with consistent variability and no trend. The correlation between Td and SI/4 was good with  $\beta = 0.9$ ,  $R = 0.84$ ,  $P < 0.01$  with no visual bias in the residual plot. (C) LV dP/dt<sub>max</sub> was only weakly correlated with SI. (D) A significant relationship between the left ventricular electrical delay (Q-LV) measured from onset of Q to the lateral electrode, at baseline, with LBBB and with RV pace. Td, time-to-peak LV dP/dt; SI, synchronicity index; LBBB, left bundle branch block; LV dP/dt<sub>max</sub>, maximum left ventricular first-order pressure derivative.

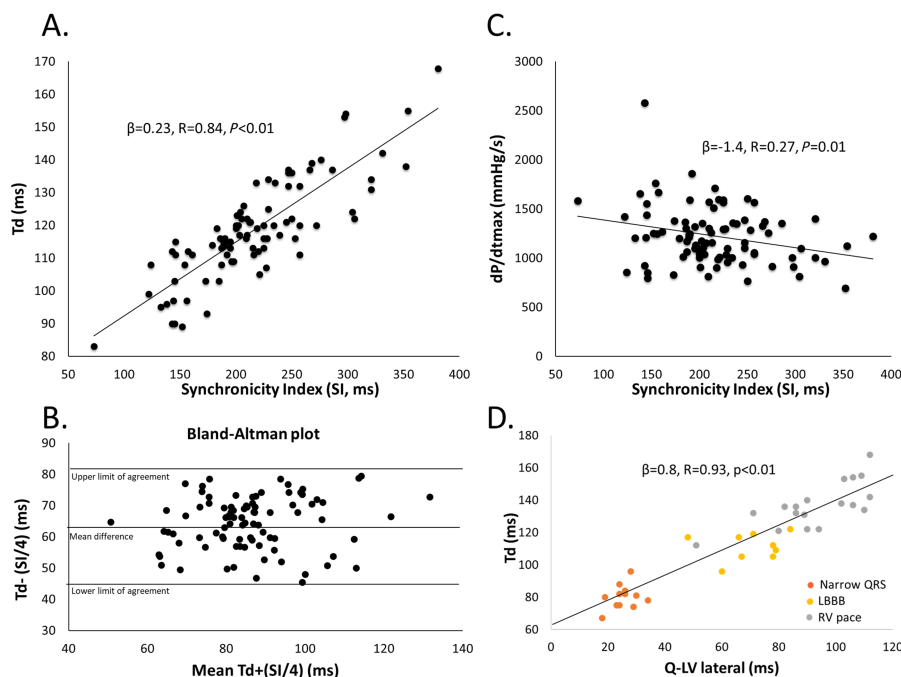


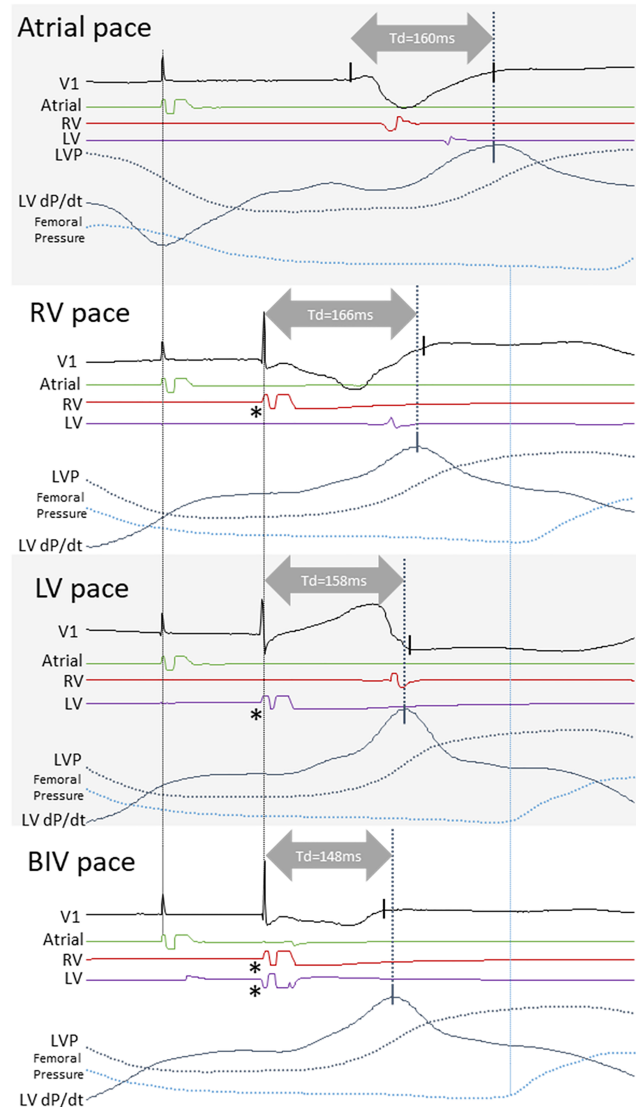
**Table 2** Baseline characteristics

	All patients (n = 45)	Responders (n = 37)	Non-responders (n = 6)	P-value
Age (years)	63 ± 10 years	62 ± 9 years	72 ± 10 years	0.02
Gender (%)				
Male	32 (71)	25 (68)	5 (83)	0.45
Weight (kg)	89 ± 18 kg	90 ± 19 kg	82 ± 7 kg	0.36
Height (cm)	164 ± 7 cm	174 ± 6 cm	178 ± 2 cm	0.22
Heart failure aetiology (%)				
Non-ischaemic	22 (49)	22 (59)	0%	
Ischaemic	23 (51)	15 (41)	100%	<0.01
Medication (%)				
ACE inhibitor/ARB	42 (93)	35 (95)	5 (83)	0.33
Beta-blocker	40 (89)	32 (87)	6 (100)	0.40
Aldosterone antagonists	28 (63)	21 (57)	4 (67)	0.71
Diuretics	28 (62)	22 (60)	5 (83)	0.30
QRS configuration (%)				
LBBB	39 (87)	35 (95)	3 (50)	<0.01
IVCD		2 (5)	3 (50)	
QRS duration	173 ± 15 ms	176 ± 15 ms	157 ± 11 ms	<0.01
NYHA class	2.5 ± 0.5	2.5 ± 0.5	2.8 ± 0.4	0.09
NYHA class II (%)	23 (51)	20 (54)	1 (17)	0.09
NYHA class III (%)	22 (49)	17 (46)	5 (83)	0.09

ACE inhibitor, angiotensin-converting enzyme inhibitor; ARB, angiotensin II receptor blocker; IVCD, intraventricular conduction disease; LBBB, left bundle branch block; NYHA, New York Heart Association.

Two patients were lost to follow-up and not included in the stratification. The P-values for comparison of responders versus non-responders are based on general linear models. Continuous variables are given as mean ± SD.

**Figure 4** Synergy from biventricular resynchronization on the timing of peak dP/dt. The panel shows atrial, RV, LV and biventricular pacing with pacing electrode EGMs, LV pressure, LV pressure derivative, and femoral artery pressure from one patient. Td is longer with RV pace than with LV pace, and without myocardial synergy between RV pace and LV pace, one would expect Td with BIV pace (which includes the two pacing electrodes) to be similar to the shorter of that from RV or LV pace; however, BIV pace shortens by 10 ms compared with LV pace demonstrating the presence of myocardial synergy resulting in an earlier pressure increase with BIV pace. Note that a long Q-LV, RV pace to LV sensed interval, and LV pace to RV sensed interval, confirming the placement of the LV electrode in a late activated region of the LV electrically distant from the RV electrode. Asterisk denotes a pacing artefact. V1, ECG lead; RV, right ventricle; LV, left ventricle; LVP, left ventricular pressure; LV dP/dt, LV pressure derivative; Td, time-to-peak LV dP/dt.



#### Acute correction of QRS duration and time-to-peak dP/dt (Td)

QRSd and Td were significantly lower in the non-responder group than in the responder group at implantation (Table 4). QRSd decreased in responders with BIVP, while Td increased with BIVP in non-responders. The corrected Td with BIVP increased by  $+12 \pm 8$  ms from baseline in non-responders, while it decreased by  $-22 \pm 3$  ms in responders ( $P < 0.01$ ).

#### Relationship between time-to-peak dP/dt (Td), QRS duration, left ventricular electrical delay (Q-LV), and reverse remodelling

We found significant linear relationships between both Td at baseline (Figure 5A) and the change in Td from baseline (Figure 5B) with the decrease in ESV at long-term (volumetric response). There was no linear relationship between QRSd at baseline and volumetric response. A significant linear relationship was found between QRSd and Td at baseline

**Table 3** Left ventricular reverse remodelling

	Responders (n = 37)	Non-responders (n = 6)	Responders versus non-responders
<b>ESV (mL)</b>			
Baseline	144 ± 12 mL	164 ± 40 mL	0.67
Follow-up	84 ± 7 mL	178 ± 47 mL	<i>P</i> < 0.01
Baseline versus follow-up	<i>P</i> < 0.01	0.82	
<b>EDV (mL)</b>			
Baseline	204 ± 14 mL	247 ± 46 mL	0.21
Follow-up	145 ± 9 mL	246 ± 54 mL	<i>P</i> < 0.01
Baseline versus follow-up	<i>P</i> < 0.01	0.98	
<b>EF biplane (%)</b>			
Baseline	31 ± 1%	35 ± 3%	0.19
Follow-up	44 ± 1%	30 ± 3%	<i>P</i> < 0.01
Baseline versus follow-up	<i>P</i> < 0.01	0.22	

EDV, end-diastolic volume; EF biplane, ejection fraction measured from echocardiographic four-chamber and two-chamber views combined; ESV, end-systolic volume.

Values are estimated marginal mean ± SEM.

**Table 4** Implantation characteristics

	Responders (n = 37)	Non-responders (n = 6)	<i>P</i> -value
<b>QRSd</b>			
Baseline	171 ± 2 ms	156 ± 6 ms	0.03
BIVP	157 ± 2 ms	167 ± 3 ms	0.12
Baseline versus	<i>P</i> < 0.01	0.15	
<b>BIVP</b>			
<b>Td</b>			
Baseline	163 ± 4 ms	121 ± 8 ms	<i>P</i> < 0.01
BIVP	156 ± 3 ms	148 ± 8 ms	0.27
Baseline versus	0.15	0.045	
<b>BIVP</b>			

BIVP, biventricular pacing; Td, time-to-peak left ventricular pressure derivative.

Values are estimated marginal mean ± SEM.

( $\beta = 0.33$ ,  $R = 0.60$ ,  $P < 0.01$ ) and after CRT ( $\beta = 0.26$ ,  $R = 0.34$ ,  $P = 0.02$ ). The ratio between Td at baseline and QRSd was linear related to Td at baseline ( $\beta = 0.004$ ,  $R = 0.85$ ,  $P < 0.01$ ), showing that the delay-to-peak LV dP/dt relative to the QRSd increase with a longer Td in patients with LBBB (Figure 5C). Similarly, Q-LV was linear related to Td at baseline ( $\beta = 0.4$ ,  $R = 0.56$ ,  $P < 0.01$ ) and with the change in Td from baseline ( $\beta = -0.4$ ,  $R = 0.44$ ,  $P < 0.01$ ).

*The proportion of responders according to QRS duration, time-to-peak dP/dt (Td) at baseline, and corrected change in time-to-peak dP/dt (Td) from baseline*

Receiver operating characteristic analysis and scatter plots (Figure 6) showed that QRSd, Q-LV, Td at baseline and corrected Td change were able to identify CRT response (QRSd Area under the curve (AUC) =  $0.76 \pm 0.11$ , 95% confidence interval 0.54–0.99,  $P < 0.05$ ; Q-LV AUC =  $0.85 \pm 0.08$ , 95% CI 0.70–1,  $P < 0.05$ ; Td at baseline AUC =  $0.92 \pm 0.06$ , 95% CI 0.79–1,  $P < 0.05$ ; corrected Td change AUC =  $0.98 \pm 0.02$ , 95% CI 0.93–1). The optimal cut-off value for corrected Td change was 3.5 ms with a sensitivity of 0.97

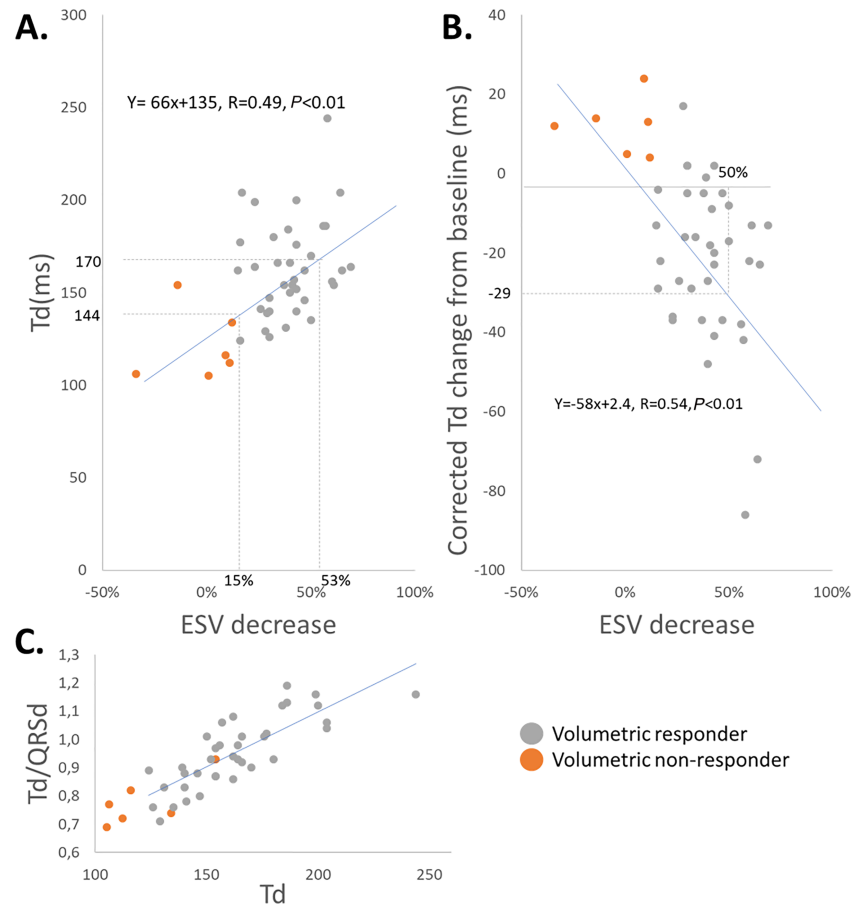
and specificity of 1.0, Td baseline it was 135 ms with a sensitivity of 0.89 and specificity of 0.83, Q-LV it was 118 ms with a sensitivity of 0.92 and specificity of 0.67, and for QRSd it was 157 ms with a sensitivity of 0.84 and specificity of 0.67.

## Discussion

Effective global force generation and rapid pressure rise are delayed without the specialized conduction system's involvement in the dyssynchronous activated ventricle.<sup>15</sup> The contraction pattern before rapid pressure rise in LBBB consists of early activation and shortening in the septal region and, instead of generating effective force, shortening occurs unopposed at low loads, and the volume of blood is pushed towards the stretching lateral wall, with low resting tension, while the mitral valve leaflets move into a closing position.<sup>16</sup> The increase in active tension with shortening in the early activated segments is counteracted and diminished by stretching. The stretch caused by active contraction elsewhere results in increased resting tension before activation in the late activated segments.<sup>17</sup> Rapid pressure rise begins as tension increases, either passively with an increased stretch or due to excitation of late activated regions.<sup>18,19</sup> Other than a delayed rapid pressure rise, the initial dyssynergistic contraction pattern with LBBB has potential effects on the total resulting myocardial force generation: (i) Increased resting tension in late activated segments may enhance active force generation in that region, and (ii) early activation and shortening in the septal region diminishes septal force generation with later resulting rebound stretch.<sup>16,18,20–22</sup> The additive effect from biventricular stimulation on the shortening of Td can be termed Synergy from biventricular stimulation (Figure 4), resulting from myocardial synergy when two regions of the heart shorten in synchrony with resulting earlier onset of rapid pressure rise. Synergy is hence specifically related to resynchronization with



**Figure 5** Crude estimates of the relationship between the baseline Td and reverse remodelling and the relationship between the corrected change in Td and reverse remodelling. (A) Scatterplot is showing the relationship between Td and ESV decrease. Stippled lines mark corresponding baseline Td values for a 15% and 53% ESV decrease—the line of equality in blue with the corresponding equation for the linear regression. (B) Scatterplot is showing the relationship between the corrected Td change from baseline and ESV decrease. The corrected change means that 15 ms is added to the baseline Td to compensate for the capture latency with pacing. The stippled lines show the corresponding value of Td change to a 50% decrease in ESV. Line of equality in blue with the corresponding equation for the linear regression. (C) Scatterplot is showing the relationship between the ratio Td/QRSD and Td. The relationship shows that a longer baseline Td is also longer relative to the baseline QRS duration. ESV, end-systolic volume; Td, time-to-peak dP/dt; QRSD, QRS duration.

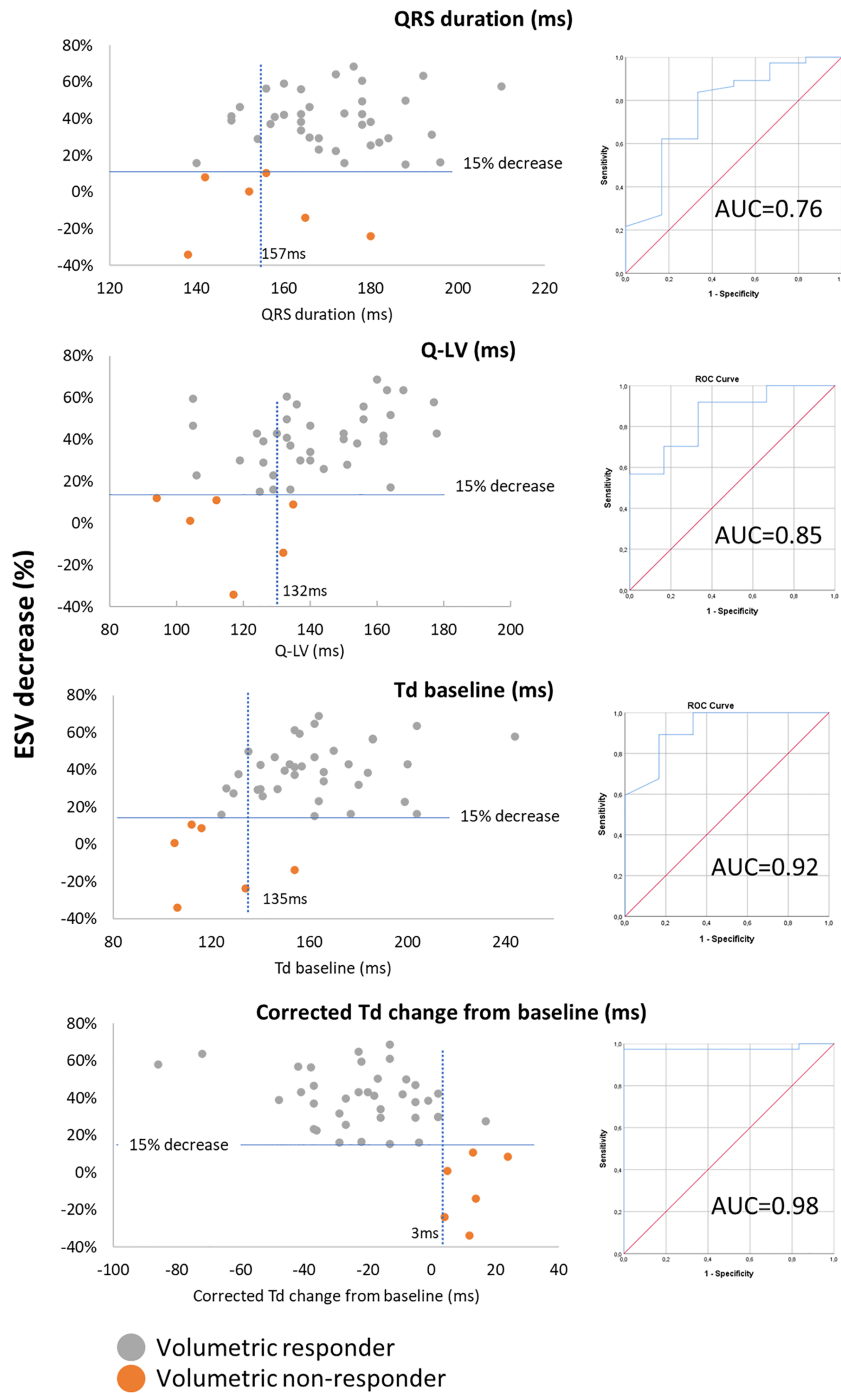


biventricular stimulation and leads to a shortening of Td, as also demonstrated in *Table 1*. Td capture the presence of both dyssynergy and synergy with resynchronization.

Td has already been assessed and suggested as a load-independent measure of contractility in patients with narrow QRS complexes, with baseline values ranging from 45 to 95 ms.<sup>23</sup> Our work shows that Td reflects dyssynergistic contraction to a more considerable extent than changes in intrinsic contractility; therefore, prolongation seen in this study is not a mere reflection of poor contractility. Td was in the range of 105 to 244 ms and significantly lower in volumetric non-responders than in responders. Higher baseline values in responders than in non-responders are in keeping with results from larger randomized trials that have used baseline preejection indices for detection of responders<sup>24,25</sup>; however, as seen in *Figure 6* and demonstrated by others,<sup>26</sup> an overlap

in baseline values are seen between volumetric responders and non-responders. Shortening of Td with CRT occurred exclusively in volumetric responders. It seems that a prolonged Td at baseline and shortening of Td with CRT, as seen in this study (*Synergy, Figure 4*), is pathognomonic for patients with reversible dysHF and that the patients without such features have other causes for HF than myocardial dyssynchrony, an issue already addressed by pioneers in CRT.<sup>27</sup> Shortening of Td with CRT has the benefit of showing a direct response from CRT compared with measuring baseline values, and it has been shown that optimization by shortening of preejection indices in device therapy is feasible.<sup>28</sup> One could easily argue that what is captured in Td is also captured in LV preejection interval (LPEI). A recent study by Moubarak *et al.* showed similar results using non-invasive measurements of LPEI.<sup>29</sup> The study included upgrades and non-LBBB patients

**Figure 6** Receiver operating characteristics. The figure displays QRS duration, Td at baseline, Q-LV and corrected Td change from baseline as predictors of long-term volumetric response to cardiac resynchronization therapy. Top panel: Scatterplot and corresponding receiver operating characteristics curve displaying QRS duration as a predictor of response to cardiac resynchronization therapy. Top middle panel: Scatterplot and corresponding receiver operating characteristics curve displaying Q-LV as a predictor of response to cardiac resynchronization therapy. Lower middle panel: Scatterplot and corresponding receiver operating characteristics curve displaying Td baseline as a predictor of response to cardiac resynchronization therapy. Lower panel: Scatterplot and corresponding receiver operating characteristics curve displaying corrected Td change from baseline as a predictor of response to cardiac resynchronization therapy. ESV, end-systolic volume; Q-LV, left ventricular electrical delay; Td, time-to-peak dp/dt; AUC, area under the curve.



but showed lower LPEI in volumetric non-responders than responders at baseline, and like in our data, an increase in LPEI in non-responders. The LPEI study results showed a significantly higher response rate among patients with non-ischaemic cardiomyopathy and a 16 ms decrease in LPEI with CRT (85% response) compared with patients with an ischaemic disease without a decrease in LPEI (36% response).<sup>29</sup> LPEI is measured during echocardiographic assessment with single-channel ECG that may be a source of error; however, inter- and intraobserver variability of <7% have been found.<sup>24,30</sup> The relationship between QRSd and QRS morphology may be necessary for evaluating baseline preejection indices as there may be other causes for prolongation of Td than dyssynchrony. Besides, certain features need to be considered before measuring the response to CRT with LPEI or Td that may preclude results. Knowledge of intrinsic AV-interval is required when measuring Td to ensure that BIVP occurs with an AV-interval shorter than the intrinsic AV-interval so that the timing of Td results from BIVP rather than from atrial stimulation that conducts through to the ventricles. Knowledge of the pacing electrode positions is also essential as this may impact myocardial contraction patterns and the resulting shortening of Td. The knowledge of the resulting QRS complex morphology from BIVP is required to avoid erroneous measurements from paced beats with loss of capture from either of the electrodes. In addition, comparing Td from paced and intrinsic beats require correction for the pace-to-capture latency that may result in erroneous classification of the effects from CRT when comparing *de novo* CRT implantations and upgrades. Pace-to-capture latency can be analysed from the resulting EGMs from the RV and LV electrodes and the QRS-complex, as shown in *Figure 2*, and would typically be in the range of 15 ms as found in this study. Comparison of Td should always be performed at equal heart rates to avoid changes in intrinsic AV-conduction times. Identification of pacing from within a scar, as seen in the Supporting Information, *Figure S2*, requires thorough examination of EGMs, ECGs and resulting Td. When searching for the optimal lead position to shorten Td the most, one should probably utilize known clinical markers as Q-LV, latest mechanical activated area, distance from scar, and one may include quadripolar leads or guidewires designed for pacing for mapping purposes.

### Disease modification and mortality associated with cardiac resynchronization therapy

How to determine response to CRT has been debated over the past decades, and it has been argued that similar to drug treatment, one may accept various treatment effects in the population treated.<sup>2</sup> However, left ventricular remodelling with ESV reduction at more than 6 months is a strong determinant for all-cause mortality and cardiovascular mortality

after CRT.<sup>6</sup> To analyse a biomarker's performance, such as Td, we felt that an objective endpoint like ESV reduction was required. We acknowledge that patients may have valuable CRT benefits beyond mortality reduction, like symptomatic relief and reduced hospitalizations. Despite selecting patients according to current guidelines, a significant number of patients may still get worse after CRT with progressive disease.<sup>1</sup> Failure to shorten Td in such patients may indicate that dysHF is not present, or it may result from inappropriate placement of the pacing leads. A viable approach for optimizing the LV lead position could be to target areas where Td shortens the most. Shortening of Td could be used to confirm effective resynchronization when selecting pacing sites based on classical criteria for placement, like interlead distance, Q-LV, late mechanical contraction, and scar location.

Our study shows that, even in the patients most likely to respond to CRT,<sup>31</sup> we can detect patients with progression of the disease or potential adverse effects from CRT based on the response of Td to pacing (*Figures 5 and 6*). The binary classification into non-responders and responders does not consider this effect; however, we may improve our future understanding of the mechanisms resulting in response to CRT by including the presence or absence of synergy from biventricular stimulation in the analyses.

Optimization of lead positioning utilizing Td as a biomarker could be the path to improve treatment in patients with dysHF to induce reverse remodelling, stop disease progression and reduce overall mortality. In a future scenario, one may expect that patients that do not present with Synergy from CRT (no shortening of Td compared with baseline), despite all available efforts and techniques, should be evaluated for implantable cardioverter implantation and be followed by HF specialist to take advantage of optimal and novel HF treatment. What to do in patients who experience a significant ventricular pacing burden after optimizing atrioventricular (AV)-synchrony to achieve better haemodynamics with a pacemaker remains unanswered by this study. In our opinion, two options exist for patients without demonstrable Synergy from CRT; one is to apply BIVP in a configuration that shortens Td the most or to apply physiological pacing that is resulting in an unchanged Td compared with baseline. In such patients, haemodynamic and symptomatic benefits from improved AV-synchrony may outweigh the detrimental effects of introducing dyssynchrony by pacing.<sup>32</sup>

### Underlying substrate for dyssynchronous heart failure and response to cardiac resynchronization therapy

The mechanical mechanisms associated with dysHF seem to be linked to left ventricular dyssynergistic contraction patterns resulting from dyssynchronous electrical activation leading to a shift in regional load during early myocardial

contraction.<sup>33–35</sup> As demonstrated in *figure 4*, synergy seems to be a phenomenon linked to CRT that characterizes patients responding to CRT. If an electrical cardiac conduction defect is linked to a disease, one would expect that removing the defect would also remove the associated disease. As such, one could argue that synergy is the required hallmark to demonstrate the effect of removing the conduction disease with BIVP in dysHF. The altered myocardial contraction pattern resulting from the conduction block is likely the driver of the cardiac remodelling processes, and hence, removing the conduction block should promote reversal of the remodelling processes. Contraction patterns present in patients with LBBB that are modified with CRT may also be modified by ischaemia or stiffening of cardiac walls.<sup>36</sup> Hence, the underlying substrate is potentially modifiable by different mechanisms. A patient with an electrical substrate may not experience any effects from CRT because of co-existing non-electrical substrates. Therefore, these patients are unlikely to show synergy as a response to pacing. In addition to LBBB, artificial stimulation of the myocardium with a pacemaker may introduce dyssynergistic contraction patterns similar to that resulting from LBBB, and pacing may be harmful in patients with and without a prevailing dyssynchronous substrate.<sup>24,37–40</sup> Therefore, it is critical to ensure that heart failure patients have dyssynergistic contraction patterns before considering CRT and that they are responding with synergy when resynchronization treatment is implemented (*Figure 4*, confirming the presence of preexisting dyssynergy and resulting synergy).

### QRS duration, left ventricular electrical delay (Q-LV), and time-to-peak dP/dt (Td)

Prolonged QRSd is a prerequisite for CRT, and shortening with CRT is associated with a favourable outcome.<sup>41,42</sup> QRSd is scaled to heart and body size, and a strict absolute cut-off might not be appropriate without considering body size.<sup>4,43,44</sup> LBBB in dogs is typically present with a QRSd of 100–110 ms, while in humans, dependent on body size, it is above 130–150 ms.<sup>11</sup> QRSd may also reflect electrical delays not affecting left ventricular contraction patterns as typically seen in right bundle branch block.<sup>45</sup> QRSd beyond 130 ms without considering other markers of electrical activation is unlikely to produce a viable cut-off for patient selection. Careful evaluation of electrical activation patterns and QRS morphology may better reflect the underlying electrical substrate.<sup>46</sup> Q-LV similar to QRSd, as expected in patients with LBBB, associated with Td at baseline in our study, and it was also associated with the decrease in Td from baseline with BIVP and performed better for detection of non-responders than QRSd (*Figure 6*). Q-LV largely depends on electrode position and underlying substrate and is linked to QRS duration in LBBB.

The timing of cardiac events is dependent on body size, heart rate, and contractility, and as demonstrated in this study—dyssynchrony. Consequently, both QRSd and Td are expected to be different among patients with different body constitutions. In addition, myocardial distensibility, which allows deformation prior to Td, may also play a role in the relationship between Td and QRSd, as a more extended baseline Td relative to the QRS complex is associated with more subsequent shortening of Td with CRT (*Figure 5*).

### Future perspectives

Td could find its place as a biomarker to identify dysHF and to help optimize CRT. A biomarker needs to be robust, operator-independent and accurate while delivering high sensitivity and specificity in detecting disease. It is prudent that a biomarker is measured in its most robust utility in larger sized clinical trials. Td should be measured invasively, in the most robust fashion, with a pressure sensor in the LV until enough clinical evidence has been collected to support or reject its ability to function as a biomarker for the purpose. An LV catheter with a combined pressure sensor and electrodes for biventricular endocardial stimulation could potentially clarify if synergy from pacing is present or not, even before placing permanent pacing leads into the heart. Once the biomarker is established, one may search for less invasive alternatives to replace the method with similar robust and operator-independent markers; however, non-invasive surrogates are likely less robust and less accurate to deliver what is required as a basis for critical clinical decisions regarding CRT. More effective therapy resulting from the measurement of Td in patients could promote cost-effectiveness and CRT utilization and help close existing knowledge gaps in the current CRT practice.<sup>2,47</sup> We have shown how a prolonged Td and shortening with resynchronization therapy identifies patients with long-term beneficial effects from CRT in a homogeneous group of patients. It seems even more critical to identify volumetric responders among patients with an ischaemic myocardial disease and intraventricular conduction delays with a lower responder rate.

### Limitations

This study was a single-centre observational study with a small sample size of a relatively homogeneous population. Therefore, the results may not be valid in a general population with a widened QRS complex without typical LBBB or patients with a significant scar burden. Future studies are required

## Conclusion

A prolonged Td that shortens with BIVP (synergy from BIV pacing) characterize patients with dyssynchronous heart failure and long-term reverse volumetric remodelling and has the potential to be utilized as a biomarker for precision medicine in cardiac resynchronization therapy.

## Acknowledgement

We want to acknowledge the significant contribution to the clinical study's organization by Mr Lars Ove Gammelsrud, Medtronic Inc.

## Conflict of interest

None declared.

## Funding

M.V. funded by EU's Horizon 2020 research and innovation programme under the Marie Skłodowska-Curie grant agreement No. 764738; Personalized In-silico Cardiology (PIC). H.

H.O. was funded by Norwegian South-East Health Authorities and Center for Cardiological Innovation, Oslo University Hospital.

## Conflict of interest

H.H.O. had an honorary from Abbott Medical, Stockholder Pacertool, and patent applications within the field of cardiac resynchronization therapy. R.C. is an employee of Medtronic Inc, Stockholder Medtronic Inc. T.H. and E.K. have no conflict of interest.

## Supporting information

Additional supporting information may be found online in the Supporting Information section at the end of the article.

**Figure S1.** Left ventricular electrode positions and survival. **Figure S2.** Left ventricular fusion pacing with intrinsic right ventricular activation compared to intrinsic activation in a patient with LBBB and ischemic heart disease (occluded RCA and Cx, and a Fractionated Flow Reserve in LAD of 0.67).

## References

1. Barra S, Duehmke R, Providencia R, Narayanan K, Reitan C, Roubicek T, Polasek R, Chow A, Defaye P, Fauchier L, Piot O, Deharo JC, Sadoul N, Klug D, Garcia R, Dockrill S, Virdee M, Pettit S, Agarwal S, Borgquist R, Marijon E, Boveda S. Very long-term survival and late sudden cardiac death in cardiac resynchronization therapy patients. *Eur Heart J*. 2019; **40**: 2121–2127.
2. Mullens W, Auricchio A, Martens P, Witte K, Cowie MR, Delgado V, Dickstein K, Linde C, Vernooy K, Leyva F, Bauersachs J, Israel CW, Lund L, Donal E, Boriani G, Jaarsma T, Berruezo A, Traykov V, Yousef Z, Kalarus Z, Nielsen JC, Steffel J, Vardas P, Coats A, Seferovic P, Edvardson T, Heidbuchel H, Ruschitzka F, Leclercq C. Optimized Implementation of cardiac resynchronization therapy: a call for action for referral and optimization of care. *Eur J Heart Fail* 2020; **22**: 2349–2369.
3. Leyva F, Zegard A, Okafor O, de Bono J, McNulty D, Ahmed A, Marshall H, Ray D, Qiu T. Survival after cardiac resynchronization therapy: results from 50 084 implantations. *Europace*. 2019; **21**: 754–762.
4. Biton Y, Kutyla V, Cygankiewicz I, Goldenberg I, Klein H, McNitt S, Polonsky B, Ruwald AC, Ruwald MH, Moss AJ, Zareba W. Relation of QRS duration to clinical benefit of cardiac resynchronization therapy in mild heart failure patients without left bundle branch block: the multicenter automatic defibrillator implantation trial with cardiac resynchronization therapy substudy. *Circ Heart Fail*. 2016; **9**: e002667.
5. Goldstein RE, Haigney MC, Krone RJ, McNitt S, Zareba W, Moss AJ. Differing effects of cardiac resynchronization therapy on long-term mortality in patient subgroups of MADIT-CRT defined by baseline conduction and 1-year post-treatment left ventricular remodeling. *Heart Rhythm*. 2013; **10**: 366–373.
6. Naqvi SY, Jawaaid A, Vermilye K, Biering-Sorensen T, Goldenberg I, Zareba W, McNitt S, Polonsky B, Solomon SD, Kutyla V. Left ventricular reverse remodeling in cardiac resynchronization therapy and long-term outcomes. *JACC Clin Electrophysiol*. 2019; **5**: 1001–1010.
7. Kawata H, Bao H, Curtis JP, Minges KE, Mitiku T, Birgersdotter-Green U, Feld GK, Hsu JC. Cardiac resynchronization defibrillator therapy for nonspecific intraventricular conduction delay versus right bundle branch block. *J Am Coll Cardiol*. 2019; **73**: 3082–3099.
8. Leyva F, Nisam S, Auricchio A. 20 years of cardiac resynchronization therapy. *J Am Coll Cardiol*. 2014; **64**: 1047–1058.
9. Salden OAE, Vernooy K, van Stipdonk AMW, Cramer MJ, Prinzen FW, Meine M. Strategies to improve selection of patients without typical left bundle branch block for cardiac resynchronization therapy. *JACC Clin Electrophysiol*. 2020; **6**: 129–142.
10. Urheim S, Edvardson T, Torp H, Angelsen B, Smiseth OA. Myocardial strain by doppler echocardiography. validation of a new method to quantify regional myocardial function. *Circulation* 2000; **102**: 1158–1164.
11. Liu L, Tockman B, Girouard S, Pastore J, Walcott G, KenKnight B, Spinelli J. Left ventricular resynchronization therapy in a canine model of left bundle branch



- block. *Am J Physiol Heart Circ Physiol* 2002; **282**: H2238–H2244.
12. Vecera J, Penicka M, Eriksen M, Russell K, Bartunek J, Vanderheyden M, Smiseth OA. Wasted septal work in left ventricular dyssynchrony: a novel principle to predict response to cardiac resynchronization therapy. *Eur Heart J Cardiovasc Imaging* 2016; **17**: 624–632.
  13. Strauss DG, Selvester RH, Wagner GS. Defining left bundle branch block in the era of cardiac resynchronization therapy. *Am J Cardiol* 2011; **107**: 927–934.
  14. Jang H, Conklin DJ, Kong M. Piecewise nonlinear mixed-effects models for modeling cardiac function and assessing treatment effects. *Comput Methods Programs Biomed* 2013; **110**: 240–252.
  15. Wiggers CJ. The muscular reactions of the mammalian ventricles to artificial surface stimuli. *Am J Physiol-Legacy Content* 1925; **73**: 346–378.
  16. Remme EW, Niederer S, Gjesdal O, Russell K, Hyde ER, Smith N, Smiseth OA. Factors determining the magnitude of the pre-ejection leftward septal motion in left bundle branch block. *Europace* 2016; **18**: 1905–1913.
  17. Byrne MJ, Helm RH, Daya S, Osman NF, Halperin HR, Berger RD, Kass DA, Lardo AC. Diminished left ventricular dyssynchrony and impact of resynchronization in failing hearts with right versus left bundle branch block. *J Am Coll Cardiol* 2007; **50**: 1484–1490.
  18. De Boeck BW, Teske AJ, Meine M, Leenders GE, Cramer MJ, Prinzen FW, Doevendans PA. Septal rebound stretch reflects the functional substrate to cardiac resynchronization therapy and predicts volumetric and neurohormonal response. *Eur J Heart Fail*. 2009; **11**: 863–871.
  19. Prinzen FW, Hunter WC, Wyman BT, McVeigh ER. Mapping of regional myocardial strain and work during ventricular pacing: experimental study using magnetic resonance imaging tagging. *J Am Coll Cardiol*. 1999; **33**: 1735–1742.
  20. Brady AJ. Onset of contractility in cardiac muscle. *J Physiol* 1966; **184**: 560–580.
  21. Remme EW, Lyseggen E, Helle-Valle T, Opdahl A, Pettersen E, Vartdal T, Ragnarsson A, Ljosland M, Ihlen H, Edvardsen T, Smiseth OA. Mechanisms of pre-ejection and post-ejection velocity spikes in left ventricular myocardium: interaction between wall deformation and valve events. *Circulation* 2008; **118**: 373–380.
  22. Russell K, Smiseth OA, Gjesdal O, Qvigstad E, Norseng PA, Sjaastad I, Opdahl A, Skulstad H, Edvardsen T, Remme EW. Mechanism of prolonged electromechanical delay in late activated myocardium during left bundle branch block. *Am J Physiol Heart Circ Physiol* 2011; **301**: H2334–H2343.
  23. Adler D, Monrad ES, Hess OM, Kraysenbuehl HP, Sonnenblick EH. Time to dp/dt (max), a useful index for evaluation of contractility in the catheterization laboratory. *Clin Cardiol*. 1996; **19**: 397–403.
  24. Chung ES, Leon AR, Tavazzi L, Sun JP, Nihoyannopoulos P, Merlino J, Abraham WT, Ghio S, Leclercq C, Bax JJ, Yu CM, Gorcsan J 3rd, St John Sutton M, De Sutter J, Murillo J. Results of the Predictors of Response to CRT (PROSPECT) trial. *Circulation*. 2008; **117**: 2608–2616.
  25. Cleland JG, Daubert JC, Erdmann E, Freemantle N, Gras D, Kappenberger L, Tavazzi L and Cardiac Resynchronization-Heart Failure Study I. The effect of cardiac resynchronization on morbidity and mortality in heart failure. *N Engl J Med*. 2005; **352**: 1539–1549.
  26. Bordachar P, Lafitte S, Reant P, Reuter S, Clementy J, Mletzko RU, Siegel RM, Goscinska-Bis K, Bowes R, Morgan J, Benard S, Leclercq C. Low value of simple echocardiographic indices of ventricular dyssynchrony in predicting the response to cardiac resynchronization therapy. *Eur J Heart Fail*. 2010; **12**: 588–592.
  27. Cazeau S, Ritter P, Lazarus A, Gras D, Backdach H, Mundler O, Mugica J. Multisite pacing for end-stage heart failure: early experience. *Pacing Clin Electrophysiol: PACE*. 1996; **19**: 1748–1757.
  28. Moubarak G, Ritter P, Daubert JC, Cazeau S. First experience of intraoperative echocardiography-guided optimization of cardiac resynchronization therapy delivery. *Arch Cardiovasc Dis* 2014; **107**: 169–177.
  29. Moubarak G, Viart G, Anselme F. Acute correction of electromechanical dyssynchrony and response to cardiac resynchronization therapy. *ESC Heart Fail*. 2020; **7**: 1302–1308.
  30. Cazeau S, Bordachar P, Jauvert G, Lazarus A, Alonso C, Vandrell MC, Mugica J, Ritter P. Echocardiographic modeling of cardiac dyssynchrony before and during multisite stimulation: a prospective study. *Pacing Clin Electrophysiol: PACE*. 2003; **26**: 137–143.
  31. Stabile G, Pepi P, Palmisano P, D'Onofrio A, De Simone A, Caico SI, Pecora D, Rapacciuolo A, Arena G, Marini M, Pieragnoli P, Badolati S, Savarese G, Maglia G, Iuliano A, Botto GL, Malacrida M, Bertaglia E. Adherence to 2016 European Society of Cardiology guidelines predicts outcome in a large real-world population of heart failure patients requiring cardiac resynchronization therapy. *Heart Rhythm*. 2018; **15**: 1675–1682.
  32. Stockburger M, Moss AJ, Klein HU, Zareba W, Goldenberg I, Biton Y, McNitt S, Kutyla V. Sustained clinical benefit of cardiac resynchronization therapy in non-LBBB patients with prolonged PR-interval: MADIT-CRT long-term follow-up. *Clin Res Cardiol* 2016; **105**: 944–952.
  33. Duchenne J, Aalen JM, Cvijic M, Larsen CK, Galli E, Bezy S, Beela AS, Unlu S, Pagourelis ED, Winter S, Hopp E, Kongsgard E, Donal E, Fehske W, Smiseth OA, Voigt JU. Acute redistribution of regional left ventricular work by cardiac resynchronization therapy determines long-term remodelling. *Eur Heart J Cardiovasc Imaging* 2020; **21**: 619–628.
  34. Salden OAE, Zweerink A, Wouters P, Allaart CP, Geelhoed B, de Lange FJ, Maass AH, Rienstra M, Vernooij K, Vos MA, Meine M, Prinzen FW, Cramer MJ. The value of septal rebound stretch analysis for the prediction of volumetric response to cardiac resynchronization therapy. *Eur Heart J Cardiovasc Imaging* 2021; **22**: 37–45.
  35. Wouters PC, Leenders GE, Cramer MJ, Meine M, Prinzen FW, Doevendans PA, De Boeck BWL. Acute recoordination rather than functional hemodynamic improvement determines reverse remodelling by cardiac resynchronization therapy. *Int J Cardiovasc Imaging* 2021.
  36. Aalen JM, Remme EW, Larsen CK, Andersen OS, Krogh M, Duchenne J, Hopp E, Ross S, Beela AS, Kongsgard E, Bergsland J, Odland HH, Skulstad H, Opdahl A, Voigt JU, Smiseth OA. Mechanism of abnormal septal motion in left bundle branch block: role of left Ventricular Wall interactions and myocardial scar. *JACC Cardiovasc Imaging* 2019; **12**: 2402–2413.
  37. Ruschitzka F, Abraham WT, Singh JP, Bax JJ, Borer JS, Brugada J, Dickstein K, Ford I, Gorcsan J 3rd, Gras D, Krum H, Sogaard P, Holzmeister J, Echo CRTSG. Cardiac-resynchronization therapy in heart failure with a narrow QRS complex. *N Engl J Med*. 2013; **369**: 1395–1405.
  38. Derval N, Bordachar P, Lim HS, Sacher F, Ploux S, Laborderie J, Steendijk P, Deplagne A, Ritter P, Garrigue S, Denis A, Hocini M, Haissaguerre M, Clementy J, Jais P. Impact of pacing site on QRS duration and its relationship to hemodynamic response in cardiac resynchronization therapy for congestive heart failure. *J Cardiovasc Electrophysiol* 2014; **25**: 1012–1020.
  39. Ploux S, Eschalier R, Whinnett ZI, Lumens J, Derval N, Sacher F, Hocini M, Jais P, Dubois R, Ritter P, Haissaguerre M, Wilkoff BL, Francis DP, Bordachar P. Electrical dyssynchrony induced by biventricular pacing: implications for patient selection and therapy improvement. *Heart Rhythm*. 2015; **12**: 782–791.
  40. Vidula H, Kutyla V, McNitt S, Goldenberg I, Solomon SD, Moss AJ, Zareba W. Long-term survival of patients with left bundle branch block who are hypo-responders to cardiac resynchronization therapy. *Am J Cardiol* 2017; **120**: 825–830.
  41. Korantzopoulos P, Zhang Z, Li G, Fragakis N, Liu T. Meta-analysis of the usefulness of change in QRS width to predict response to cardiac

- resynchronization therapy. *Am J Cardiol* 2016; **118**: 1368–1373.
42. Okafor O, Zegard A, van Dam P, Stegemann B, Qiu T, Marshall H, Leyva F. Changes in QRS area and QRS duration after cardiac resynchronization therapy predict cardiac mortality, heart failure hospitalizations, and ventricular arrhythmias. *J Am Heart Assoc* 2019; **8**: e013539.
43. Rickard J, Baranowski B, Grimm RA, Niebauer M, Varma N, Tang WHW, Wilkoff BL. Left ventricular size does not modify the effect of QRS duration in predicting response to cardiac resynchronization therapy. *Pacing Clin Electrophysiol: PACE* 2017; **40**: 482–487.
44. Varma N, Lappe J, He J, Niebauer M, Manne M, Tchou P. Sex-specific response to cardiac resynchronization therapy: effect of left ventricular size and QRS duration in left bundle branch block. *JACC Clin Electrophysiol* 2017; **3**: 844–853.
45. Poole JE, Singh JP, Birgersdotter-Green U. QRS duration or QRS morphology: what really matters in cardiac resynchronization Therapy? *J Am Coll Cardiol* 2016; **67**: 1104–1117.
46. van der Bijl P, Khidir M, Leung M, Mertens B, Ajmone Marsan N, Delgado V, Bax JJ. Impact of QRS complex duration and morphology on left ventricular reverse remodelling and left ventricular function improvement after cardiac resynchronization therapy. *Eur J Heart Fail* 2017; **19**: 1145–1151.
47. Fudim M, Dalgaard F, Al-Khatib SM, Friedman DJ, Lallinger K, Abraham WT, Cleland JGF, Curtis AB, Gold MR, Kutiyifa V, Linde C, Schaber DE, Tang A, Ali-Ahmed F, Goldstein SA, Kaufman B, Fortman R, Davis JK, Inoue LYT, Sanders GD. Future research prioritization in cardiac resynchronization therapy. *Am Heart J.* 2020; **223**: 48–58.